

A comparison of implementation of linear and nonlinear constitutive models in numerical analysis of layered flexible pavement

Behzad Ghadimi & Hamid Nikraz

To cite this article: Behzad Ghadimi & Hamid Nikraz (2016): A comparison of implementation of linear and nonlinear constitutive models in numerical analysis of layered flexible pavement, Road Materials and Pavement Design, DOI: [10.1080/14680629.2016.1182055](https://doi.org/10.1080/14680629.2016.1182055)

To link to this article: <http://dx.doi.org/10.1080/14680629.2016.1182055>



Published online: 11 May 2016.



Submit your article to this journal [↗](#)



Article views: 22



View related articles [↗](#)



View Crossmark data [↗](#)

A comparison of implementation of linear and nonlinear constitutive models in numerical analysis of layered flexible pavement

Behzad Ghadimi*  and Hamid Nikraz

Civil Engineering Department, Curtin University, Perth, WA, Australia

(Received 28 October 2013; accepted 18 April 2016)

It is generally accepted among pavement engineers that the granular layers in flexible pavement behave in a nonlinear mechanical way. Existing literature documents different constitutive equations to model this nonlinearity. This paper compares four well-known constitutive models: linear elastic, $K - \theta$, Uzan–Witezak and Lade–Nelson. In the first stages of numerical simulation, three static linear elastic models were constructed in CIRCLY, KENLAYER and ABAQUS and the results of the analysis were compared with one another. Following this, three-dimensional models were constructed in ABAQUS, and the four constitutive models were implemented for use in the finite-element model. Three sets of material parameters were considered for the analysis. The results calculated from each model were presented and compared and consisted of the following: surface deflection under loading wheels, tensile strain at the bottom of an asphalt layer, and vertical strain and vertical stress at the top of the subgrade layers. The development of the elastic modulus and vertical stress in the base layer was also investigated and the contours of the vertical elastic modulus are presented.

Keywords: flexible pavement; ABAQUS; CIRCLY; KENLAYER; nonlinear; numerical modelling

Introduction

The main purpose of flexible pavement design is to minimise the surface deflection caused by any source of damage such as rutting or fatigue. One of the contributors to this damage is the mechanical behaviour of granular layers (base, subbase and subgrade); expressed in design codes in terms of stress, strain and displacement (AASHTO, 1993; AUSTRROADS, 2004). Therefore, estimating these parameters is essential in the design of pavement structure.

The estimation of parameters can be carried out by utilising experimentally developed equations, based on laboratory or field results. Although this approach can be simple and useable in specific cases, the extrapolation of these equations to altered conditions such as different environments, different loading conditions and different material types may not be valid.

An alternative to using the above-mentioned equations may be found in the utilisation of numerical analysis to estimate the critical parameters. Recently, advancing computer technology has created increased interest in this technique from pavement researchers. Numerical models can be easily developed for and adapted to different conditions. However, the estimated values must be validated in practical cases.

*Corresponding author. Email: behzad.ghadimi@curtin.edu.au

The numerical modelling of pavement granular materials considers two major methods. The first is a simple method which assumes linear elasticity, while the second attempts to consider the stress dependency of granular materials which lead to nonlinear elastic behaviour. The current study will compare the results of linear elasticity with three well-known nonlinear constitutive models in the numerical modelling of a sample of a three-layered flexible pavement system.

One of the useful and simple approaches that have been widely used in the numerical simulation of flexible pavement design is to assume linear elastic behaviour in the material under study. Assuming this elastic behaviour, the Boussinesq theory for elastic half-space can be applied. Burmister has investigated such an approach for two-layered pavement structures (Burmister, Palmer, Barber, Casagrande, & Middlebrooks, 1943) and other layered soil problems (Burmister, 1945). By manipulating linear elastic theory, the stress, strain and displacement in all points of the medium can be calculated (Huang, 1993). Based on this assumption, different commercial programmes have been developed. CIRCLY (Wardle, Youdale, & Rodway, 2003) and KENLAYER (Huang, 1993) are two programmes which have been widely used among pavement engineers. These programmes are mainly used to validate the initial results of more complex calculation procedures (such as the finite-element procedure). This may be seen in such studies as those conducted by Hadi and Symons (1996) where the CIRCLY programme was used to compare results with the finite-element models constructed in MSC/NASTRAN and STRAND. CIRCLY has also been used by Tutumluer, Little, and Kim (2003) in comparison with GT-PAVE for cross-anisotropic materials. In 2006, Gedafa (2006) inducted an analysis of flexible pavement using KENLAYER and HDM-4.

In the literature, the first reported use of finite element method (FEM) in flexible pavement engineering was published in Duncan, Monismith, and Wilson (1968). Following this, Huang (1969) used the FEM to calculate the nonlinear response of pavement layers. Since then, there has been a great deal of research using FEM to conduct linear, nonlinear, static and dynamic analysis (Cho, Mccullough, & Weissmann, 1996; Kim, 2007; Kim & Tutumluer, 2006; Kim, Tutumluer, & Kwon, 2009; Mallela & George, 1994; Uddin, Zhang, & Fernandez, 1994; Zaghoul & White, 1993). A commercial finite-element programme, ABAQUS (Hibbit, 2010), is one of the most well-known programmes used to investigate different types of material behaviour in this area.

While the linear elastic analysis is mainly conducted under the Hook's Law constitutive model, there are a variety of constitutive models that have been developed for the nonlinear analysis. Comprehensive reviews on the proposed nonlinear constitutive models for granular materials can be found in Rowshanzamir (1997), Kim (2007) and Bodhinayake (2008). A summary of some of the most widely used models in pavement engineering to date is reviewed in the next section. These models are $K - \theta$, Uzan (1985), Witzczak and Uzan (1988) and Lade and Nelson (1987).

Relatively recently, Hjelmstad and Taciroglu (2000), proposed a new material resilient modulus which depended upon both first and second invariants of the strain tensor rather than the stress tensor. In this study, the material stiffness matrix was also driven and the model was implemented in an ABAQUS simulation. The simulation was run for a sample triaxial model and the results were validated against the experimental values.

Taciroglu and Hjelmstad (2002), proposed a new nonlinear elastic constitutive model which coupled the shear and normal behaviour of materials in the stiffness matrix as a hyperelastic model. The authors used an analytical approach, proposing an energy function density to develop a new stress-strain relationship for the granular materials. Other analytical studies (e.g. Worku, 2012) have been conducted to estimate the modulus of foundation as a continuum medium with a fixed thickness.

Experiments can be performed to either develop a new nonlinear constitutive model or to validate the previously proposed models and evaluate their function. In this regard, the study

published by Fahey and Carter (1993) used an experimentally developed nonlinear model to connect the shear modulus of sand to induced shear stress. They then applied their proposed model to a finite-element simulation. Other major research carried out in recent years is outlined below.

González, Saleh, and Ali (2007) carried out a series of simulations, along with field measurement to evaluate the precision of nonlinear models in the prediction of mechanical responses to a given geometry. They concluded that nonlinear models are able to predict valid responses and that there is a difference among the different models. In 2009, Lee, Kim, and Kang (2009) proposed a new nonlinear model which was normalised through an experimental method. The proposed model linked the resilient modulus to induced stresses and it also stresses' time-history. The model was also applied in the finite-element theory. Attia and Abdelrahman (2011) studied the effect of different constitutive models on the resilient modulus resulting from experimental tests. In their study, they compared nine different constitutive models, including Uzan (2D and 3D), Witczak (five parameters) and $K - \theta$. Araya, Huurman, Houben, and Molenaar (2011) and Araya, Huurman, Molenaar, and Houben (2012) conducted a number of triaxial test and also carried out an ABAQUS simulation. They developed a new test, termed RL-CBR, to establish a connection between the California Bearing Ratio (CBR) and the stress-dependent resilient modulus. Mishra and Tutumluer (2012) studied the effect of aggregate shape and properties over the resilient modulus, computed from different nonlinear models. Various experimental results were investigated and compared against field observations.

These experimental investigations performed the function of providing input data for a numerical simulation. In other words, the final purpose of any constitutive model is that it be implemented in a numerical simulation and evaluated in a complete numerical analysis. In this way, a constitutive model has an impact on the final design of pavement or any other structure.

Recently there has been increasing activity from pavement researchers in the investigation of numerical simulations. For example, studies conducted by Kim (2007), Kim and Lee (2011), Kim and Tutumluer (2006, 2010) and Kim et al. (2009) investigated the validity of a nonlinear implemented modulus for the subbase, and a bilinear modulus for the subgrade in different geometries and of different material types for a multiple wheel load, as found in airfields. Sahoo and Reddy (2010) studied the effects of the nonlinear properties of granular layers on the critical response of low-volume pavement. They used Drucker–Prager's model as an elastoplastic model to predict the pavement's response. The model was constructed with the ANSYS programme and the results were validated against the linear elastic response calculated by ELAYER. Kim and Lee (2011) studied a 3D ABAQUS model assuming the Uzan–Witzack nonlinear model for the base and a bilinear model for the subgrade. They compared their results against the linear analysis. Cortes, Shin, and Santamarina (2012) implemented the nonlinear elastic model in a finite-element simulation to analyse an inverted pavement system. Wang and Al-Qadi (2013) used ABAQUS to simulate the dynamic anisotropic behaviour of granular materials under a nonlinear assumption. They used the Uzan–Witzack model for nonlinear behaviour and assumed orthotropic characteristics of the materials to model anisotropy. They compared their results against field observations and linear analysis. According to this study cross-anisotropic behaviour of granular can significantly influence the results of flexible pavement response when thin layer asphalt is used.

Although the effect of cross-anisotropic behaviour of granular materials is significant, the main focus of this study is to provide comparison basis for the different nonlinear elastic models used for simulation of the base layer of the flexible pavement structure. Therefore, in this study effects of cross-anisotropic behaviour are not simulated.

While there is an increasing trend to implement newly developed nonlinear elastic models in finite-element simulations, a study to compare the effects of these nonlinear models against each

other in a numerical analysis can reveal the final function of each model. Such a comparison provides the knowledge to choose a proper constitutive model for a specific simulation (here, for a flexible pavement system). The work done by Attia and Abdelrahman (2011) provides such a comparison in terms of experimentally calculated parameters for the different constitutive models. However, a comparison study between the final implementation of different constitutive models in numerical simulations of a sample pavement has yet to be conducted.

This study will compare the results of the implementation of four different constitutive models: (1) linear elastic, (2) $K - \theta$, (3) Uzan–Witczak and (4) Lade–Nelson.

The first step in the approach is to validate a 2D axisymmetric model. The 2D model is constructed assuming a linear constitutive model and Uzan’s (Uzan, 1985) nonlinear model. The geometry of the model is the same as that used by Kim et al. (2009). In this stage it can be seen that the effect of the boundary conditions is not significant, and the constructed model in ABAQUS is reliable. Results of the linear analysis are validated by the results of CIRCLY, KENLAER and Kim et al. (2009). The nonlinearity is then implemented into the finite-element analysis for the same geometry. ABAQUS provides a facility to implement new material models in a standard finite-element analysis through the writing of a UMAT code. The results of the nonlinear model are validated from the results of Kim et al. (2009).

In the second step, four of the constitutive models mentioned before are numerically implemented in a full 3D finite-element model. For the purposes of comparison, the material’s properties are as presented in the experimental data set by Taciroglu and Hjelmstad (2002). They presented the results of experimental tests and calculated the parameters of the various constitutive models for different material samples. Therefore, for a given sample of material, the parameters of all constitutive models are available. Moreover, nonlinearity is only assigned for the granular layers used in the base and the other two layers (asphalt layer and subgrade) are assumed to behave in a linear elastic manner. This also assists in the understanding of the role of the nonlinear constitutive model.

Finally, the results of the four constitutive models in terms of critical responses of the pavement and resultant resilient modulus are compared to each other and conclusions drawn.

Review of the nonlinear models used for granular materials

As it was reviewed in previous section, among all of nonlinear elastic models, three models have been used widely in the field of flexible pavement engineering. The first most widely used nonlinear model is known as $K - \theta$; this relates the resilient modulus (M_r) to the bulk stress as follows:

$$M_r = K \left(\frac{\theta}{P_1} \right)^n, \quad (1)$$

where K and n are the material parameters, θ is the bulk stress and P_1 is the unit pressure to normalise the θ . Seed, Chan, and Lee (1962) used this to predict the behaviour of soil under repeated loading. Following Seed, other researchers began to use this model and modified it (Hicks & Monismith, 1971). The model has the disadvantage of not including a true-stress path which is dependent upon other stress invariants. This deficit has been rectified in the proposed model by Uzan (1985). Uzan’s model relates the resilient modulus not only to the bulk stress, but also to the deviatoric stress as follows:

$$M_r = K_1 \left(\frac{\theta}{P_1} \right)^{k_2} \left(\frac{\sigma_d}{P_1} \right)^{k_3}. \quad (2)$$

Here σ_d indicates the deviatoric stress and P_1 is the unit pressure. K_1 , k_2 and k_3 are the material parameters. The Uzan model accounts for axisymmetric conditions. This model was later expanded by Witzak and Uzan (1988) to encompass full three-dimensional conditions:

$$M_r = K_1 P_0 \left(\frac{I_1}{P_0} \right)^{k_2} \left(\frac{\tau_{\text{oct}}}{P_0} \right)^{k_3}, \quad (3)$$

where I_1 and τ_{oct} are the first invariants of stress tensors and octahedral shear stress, respectively. P_0 indicates the atmospheric pressure and K_1 , k_2 and k_3 are the material parameters.

Although the above-mentioned models include the stress dependency of materials, they are mainly based on experimental observation rather than taken from a theoretical basis. As a consequence, researchers have attempted to find a theoretically based nonlinear constitutive model to simulate the nonlinear resilient modulus. One of the main analytical models of this kind originates from Lade and Nelson (1987). The authors derived a resilient model which depended upon both mean normal stress and deviatoric stress. The model is based on the concept of elastic energy and virtual work and it showed that the stiffness of the material should be dependent on both the first invariant of the stress tensor and the deviatoric stress as follows:

$$M_r = K_1 \left[\left(\frac{I_1}{P_1} \right)^2 + R \left(\frac{\tau_{\text{oct}}}{P_1} \right)^2 \right]^{k_2} \quad (4)$$

$$R = 6 \frac{1 + \nu}{1 - 2\nu}.$$

The parameters are as stated before, with ν being Poisson's ratio.

In this study the three above-mentioned nonlinear models are compared with linear elastic analysis.

Problem definition

Simulation of any assumed layered pavement structure is required at a stage before the final design. For this purpose, the numerical simulation will consider a constitutive model which can represent the behaviour of specific layer. As stated in the previous section, with the granular layer, the constitutive models can be divided in two major categories of linear elastic or nonlinear constitutive models. Problems with linear elastic constitutive models can be solved in a closed-form solution for a layered half-space. In this case, the pavement is assumed as layers of linear elastic materials lying on top of each other and there is no limit at the bottom or sides. The tyre load is applied on the top layer (asphalt layer) as a uniformly distributed pressure over a circular area (representing the tyre contact area).

In the case of nonlinear constitutive models, a closed-form solution does not exist which necessitates the application of more complex methods, such as the finite-element method. However, as can be seen from the literature cited in the previous section, it is generally accepted that the behaviour of granular materials can be described more appropriately by nonlinear equations.

In the finite-element method, a given domain (which is not infinite in any direction as assumed in a closed-form solution) is discretised to elements in which the equilibrium equation is solved. Therefore the number of elements, the geometrical boundary conditions on the sides and bottom of the model, and the materials properties should be defined. To be sure that the effect of the boundary conditions and elements on the final results are negligible, the results of linear elastic material calculated from the finite-element model should be close to those calculated from the

closed-form solution. This is the first step in the analysis conducted in this study. After validation of the results from the linear elastic material, the nonlinear constitutive equation should be coded into the finite-element programme. In this step, the same approach used by Kim and Tutumluer (2006) is manipulated to compare the results of the implementation of the constitutive equation of Uzan–Witczak (Witczak & Uzan, 1988) in ABAQUS. In this step, the approach can generally be validated.

Having the validation confirmed, the other constitutive equations are implemented in the model in the same way. To have a clear comparison of the mechanical effect of these constitutive equations in the final responses, the other layers (asphalt and subgrade) are modelled as linear elastic materials.

Finally, the results calculated from each model are compared with one another and a mechanical trend is abstracted. Although the actual values of the results depend on the layer thicknesses and material properties of the other layers, the same trend in mechanical effect can be expected from these constitutive models.

There are four critical responses of the layered flexible pavement structure which are used in pavement design: (1) the surface deflection of the asphalt layer beneath loading tyre which is an indicator of damage to the asphalt; (2) the tensile strain at the bottom of asphalt layer which is used to determine fatigue performance of the asphalt layer; (3) compressive strain; and (4) compressive stress at the top of subgrade layer which are indicators of rutting in the whole pavement structure (Huang, 1993). These failure criteria are developed based on elastic response of materials (whether linear or nonlinear elastic). In the following sections, these four critical responses are selected as comparative parameters in all the numerical simulations.

In the following sections the mathematical equation behind the coding and the flowchart of the used algorithm is presented. Properties of the constructed model in CIRCLY, KENLAYER and ABAQUS are described, and the validation of coding for linear and nonlinear models is conducted. In the next step, different constitutive models are implemented in the finite-element model and the results of the critical responses calculated from constitutive models are compared to each other. In order to understand exactly how the elastic modulus varies depending on the variation of stress in the field, the results of the stress distribution and the development of the elastic modulus are demonstrated. The contours of the elastic modulus in the plan of loading wheels and an in-depth view of the nonlinear layer are then presented and described. A final discussion to explain the major implication of the results is provided and conclusions drawn.

Mathematical background and simulation procedure

Assuming elastic behaviour, the stress and strain tensors can be related through a material stiffness matrix as follows:

$$\boldsymbol{\sigma} = \mathbf{C}\boldsymbol{\varepsilon}, \quad (5)$$

In the finite-element method, the stress and strain of the whole model is calculated in increments. In each increment a set of equations is constructed and the programme tries to solve the tensor equation (Eq. (5)) for that increment. Therefore, in the FEM, the stress–strain relationship is calculated in an incremental format as can be seen in the following equation.

$$\Delta\boldsymbol{\sigma} = \mathbf{C}\Delta\boldsymbol{\varepsilon}, \quad (6)$$

in the ABAQUS standard analysis.

The role of the constitutive model is to define the matrix \mathbf{C} , known as material tangent stiffness (also known as the material Jacobian matrix). In the ABAQUS programme, the material Jacobian matrix is calculated in each increment, as can be seen in the following equation:

$$\begin{aligned} d\Delta\boldsymbol{\sigma} &= \frac{\partial\Delta\boldsymbol{\sigma}}{\partial\Delta\boldsymbol{\epsilon}}d\Delta\boldsymbol{\epsilon}, \\ \frac{\partial\Delta\boldsymbol{\sigma}}{\partial\Delta\boldsymbol{\epsilon}} &= \mathbf{C}. \end{aligned} \quad (7)$$

Figure 1 illustrates the flowchart of numerical simulation in ABAQUS.

The definition of any new constitutive model can be implemented through updating stresses and the material Jacobian matrix in each increment according to a user-defined constitutive equation. In the linear elastic constitutive model, Hook's Law is applied, as stated in the

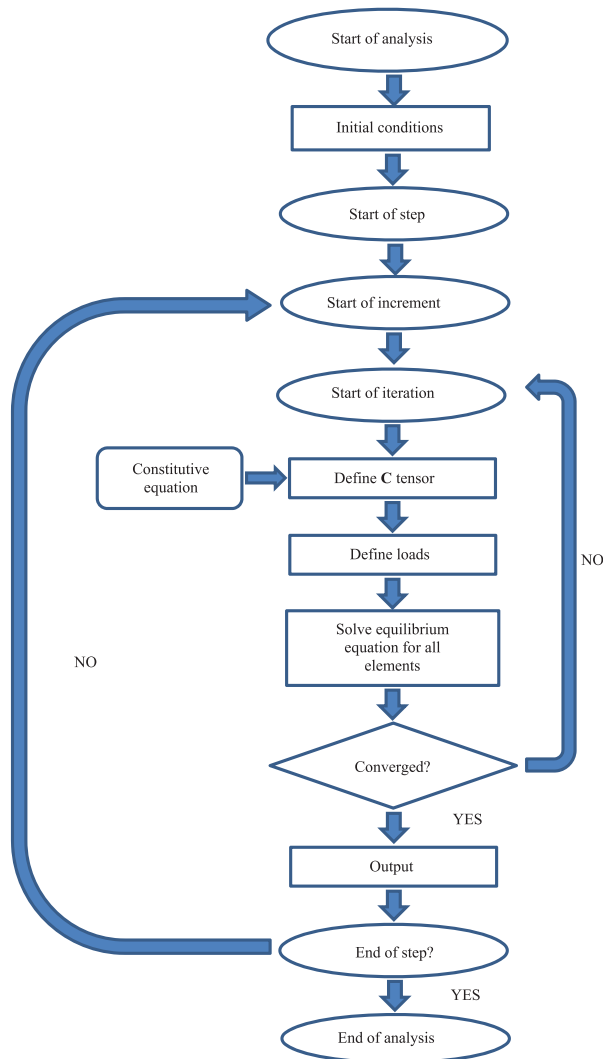


Figure 1. Flowchart of numerical simulation.

following equation:

$$\Delta\sigma = 2G\Delta\epsilon + \lambda I \Delta\epsilon : I, \quad (8)$$

where I is the identity tensor, G is the shear modulus and λ is Lamé's constant.

From the theory of elasticity it is found that:

$$\lambda = \frac{M_R \nu}{(1 + \nu)(1 - 2\nu)} \quad (9)$$

$$G = \frac{M_R}{2(1 + \nu)}.$$

where M_R is the resilient modulus. In nonlinear constitutive equations, this resilient modulus is a function of the stress tensor:

$$M_R = f(\sigma). \quad (10)$$

Therefore, in each increment the resilient modulus changes, following the change in stresses. In this study, each nonlinear constitutive equation (Eqs. (1)–(4)) is employed to calculate the material resilient modulus in a separate user-defined subroutine. Following this, the stresses and material Jacobian are updated accordingly, and finally the equilibrium equation for the whole model is solved.

Model characteristics and validation

For the purposes of verification, the same material properties and the geometry of the layers used by Kim et al. (2009) are reconstructed in CIRCLY, KENLAYER and ABAQUS. Table 1 presents the details of the model's characteristics.

The coefficient of earth pressure is assumed to be 0.5 for all of the simulations. For the finite-element model, a total of 5986 8-node biquadratic axisymmetric quadrilateral, reduced integration elements (CAX8R) are used. The boundary conditions are those of rollers on the sides and an encasté at the bottom.

To minimise the effects of the boundary conditions on the final results, the side is at a 3 m distance from the centre of the load and the bottom is situated 21 m below the loading. The loading is assumed to be a circular area (152 mm radius) and a load of 551 kPa is uniformly applied over this area. Therefore the boundary conditions are located as recommended by Kim et al. (2009).

Figure 2 illustrates the finite-element geometry, mesh distribution and contours of the vertical deflection (U2) for the linear analysis.

In Figure 3, it is clear that the linear solution to the finite-element model is quite satisfactory, and therefore the model geometry and mesh distribution effects could be considered as negligible. In the next model, the nonlinear elasticity of materials is implemented for the same geometry. The material properties are those as used by Kim et al. (2009). Here, the nonlinear constitutive

Table 1. Material properties for the linear axisymmetric model.

Layer	Thickness (mm)	Elastic modulus (MPa)	Poisson ratio
Asphalt (AC)	76	2759	0.35
Granular (Base/Subbase)	305	207	0.4
Subgrade	20,000	41.4	0.45

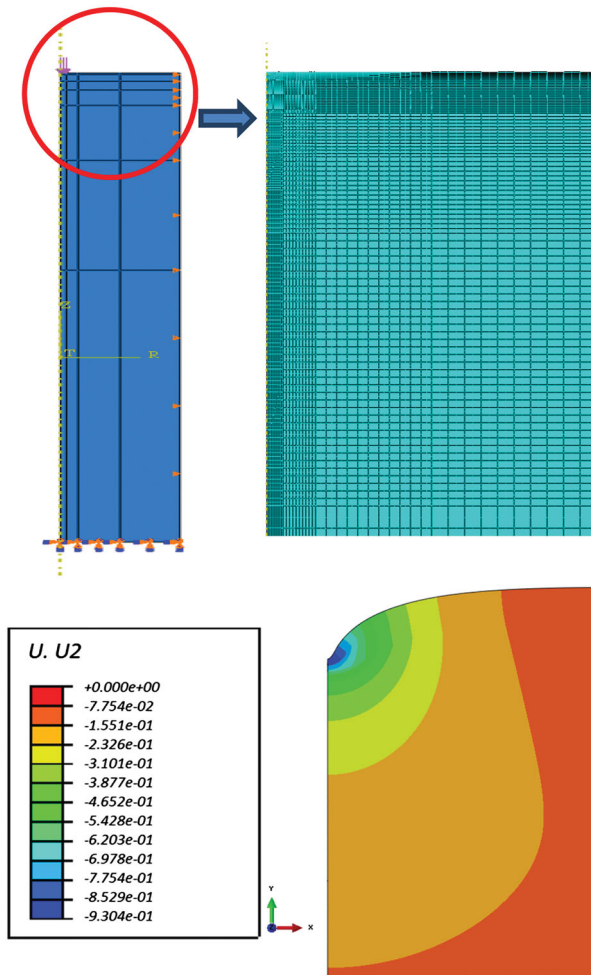


Figure 2. 2D model geometry, mesh and vertical displacement for linear analysis.

model used is Uzan – 1995 (Eq. (1)) for the axisymmetric geometry. The only nonlinear layer is the base layer and the properties of the other layers are the same as those stated in Table 1. The properties used for nonlinear materials regarding Eq. (1) are $K_1 = 4.1$ MPa, $k_2 = 0.64$ and $k_3 = 0.065$.

Table 2 summarises the results of this simulation in comparison to the results calculated by Kim et al. (2009). In this paper, compressive stress and strain are negative, while tensile stress and strain are positive.

Figure 3 compares the results of vertical deflection calculated from CIRCLY, KENLAYER and ABAQUS.

Having validated the method, a sample three-layered flexible pavement was constructed using three-dimensional geometry. Figure 4 demonstrates the geometry of the model, mesh distribution and vertical deflection (U3) for the linear analysis. The layer description of this model is indicated in Table 3.

A mesh refinement analysis was conducted until the finer mesh could not change the results of surface deflection (Figure 4). Finally a set of 104,832 8-node linear brick elements (C3D8R)

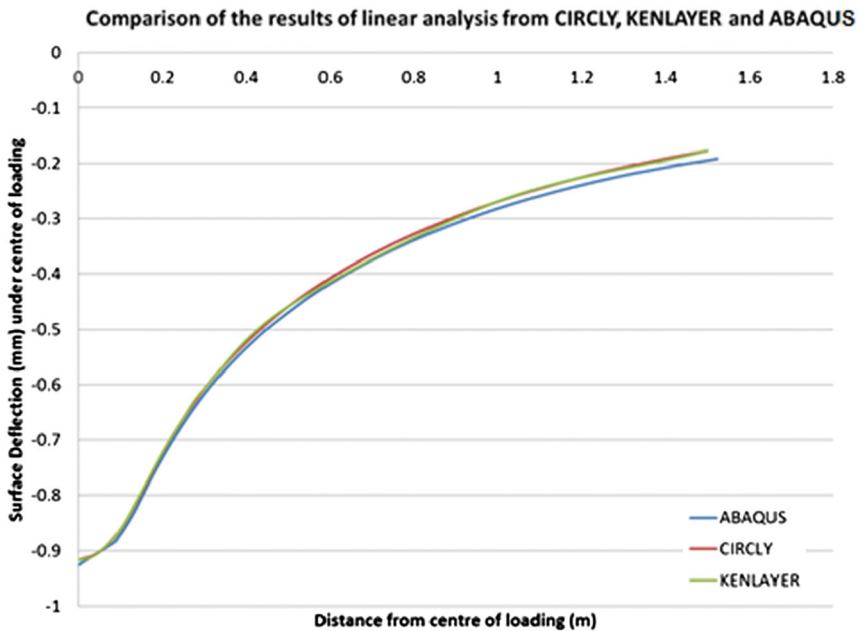


Figure 3. Comparison between results of surface deflection computed from CIRCLY, KENLAYER and ABAQUS.

Table 2. Validation of linear and nonlinear axisymmetric model.

Critical response	Linear	Kim–Tutumluer (linear)	Nonlinear	Kim–Tutumluer (nonlinear)
δ (mm) surface	-0.930	-0.930	-1.276	-1.240
ϵh (microstrains) <u>bottom of AC</u>	251	227	312	267
ϵv (microstrains) top of SG	-921	-933	-1170	-1203
σv (MPa) top of SG	-0.040	-0.041	-0.054	Not presented

was selected to construct the whole model. The load was applied as a uniform pressure of 750 kPa over two rectangular areas (representing the contact surface of the tyres) 10 cm by 10 cm. The tyres are assumed to have a distance of 1.8 m from each other.

The boundary conditions consisted of rollers on the sides and clamped at the bottom of the model. The sides were located 4 m from the closest tyre and the bottom was 25 m below the surface. This distance follows the recommendation of Kim and Tutumluer (2006) on minimising the effects of boundary conditions on the results.

The mesh is finer close to loading tyre (at the middle of the model) while coarser at the boundaries. This strategy optimises the number of elements and therefore simulation time. In Figure 4, three different layers of pavement structure are indicated with three colours (asphalt: green, base: white, subgrade: red).

Effect of different constitutive models on critical responses of layered flexible pavement

The main variables in this study were the constitutive models used for the granular base layer. As mentioned before, four types of constitutive equations were implemented. The experimental

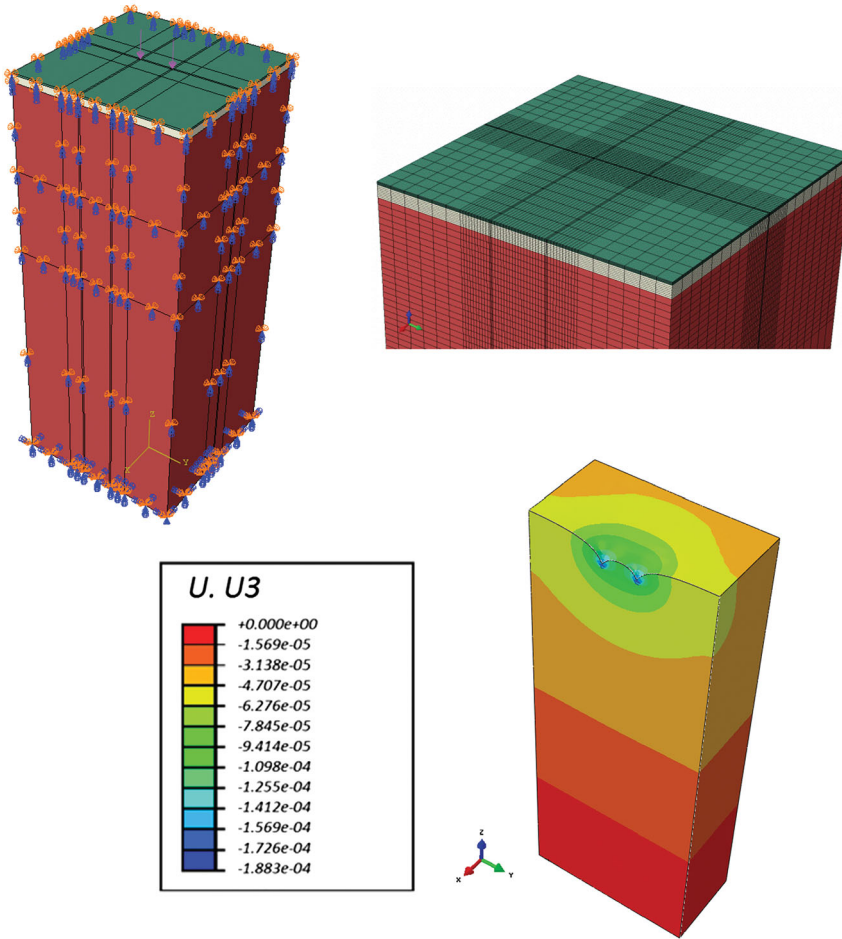


Figure 4. 3D model geometry, mesh and vertical displacement for linear analysis.

Table 3. Material properties for 3D model.

Layer	Thickness (mm)	Elastic modulus (MPa)	Poisson's ratio
Asphalt (AC)	100	2800	0.35
Granular (Base/Subbase)	400	Variable	Variable
Subgrade	24,500	50	0.3

data available from the study conducted by Taciroglu and Hjelmstad (2002) were used for the parameters of the materials. Table 4 presents these material parameters for different cases.

The effect of the constitutive models' equation can be clarified if the results of the numerical analysis are compared via the range of material input parameters. From the experimental dataset made available by Taciroglu and Hjelmstad (2002), three different samples of materials (Cases 1–3) were selected for the numerical implementation. These three cases, in effect, represented a range of materials used in the base layer for flexible pavement: good-quality materials with high density (Case 2), intermediate quality material (Case 1) and low-quality materials with lower density (Case 3). The results of the numerical implementation of the constitutive models for

Table 4. Properties of nonlinear material used in a granular base layer.

Case number	Constitutive model equations	Material parameters
Case 1 (Sample HD1)	Linear	$E = 240$ (MPa), $\nu = 0.34$
	$K - \theta$: Eq. (1)	$K = 259$ (MPa), $\nu = 0.33$, $n = 0.05$
	Uzan–Witczak: Eq. (3)	$K_1 = 459$ (MPa), $\nu = 0.33$, $k_2 = 0.03$, $k_3 = 0.27$
	Lade–Nelson: Eq. (4)	$K_1 = 242$ (MPa), $\nu = 0.33$, $k_2 = 0.13$
Case 2 (Sample HD3)	Linear	$E = 308$ (MPa), $\nu = 0.4$
	$K - \theta$: Eq. (1)	$K = 352$ (MPa), $\nu = 0.4$, $n = 0.11$
	Uzan–Witczak: Eq. (3)	$K_1 = 798$ (MPa), $\nu = 0.41$, $k_2 = -0.14$, $k_3 = 0.51$
	Lade–Nelson: Eq. (4)	$K_1 = 301$ (MPa), $\nu = 0.4$, $k_2 = 0.20$
Case 3 (Sample LD2)	Linear	$E = 179$ (MPa), $\nu = 0.36$
	$K - \theta$: Eq. (1)	$K = 226$ (MPa), $\nu = 0.34$, $n = 0.16$
	Uzan–Witczak: Eq. (3)	$K_1 = 504$ (MPa), $\nu = 0.35$, $k_2 = 0.12$, $k_3 = 0.37$
	Lade–Nelson: Eq. (4)	$K_1 = 202$ (MPa), $\nu = 0.36$, $k_2 = 0.23$

all three cases were represented in order to provide a better understanding of exactly how the constitutive models function with different types of materials. The material properties of Case 1 represent the normal average elastic modulus used for base materials. Case 2 can be assigned to hard and stiff materials and Case 3 is a representation of looser materials.

The experimental samples were selected from the one type of materials and the material parameters for each model were driven from its specific test. A complete explanation of the reliability of these parameters is presented in the work of Taciroglu and Hjelmstad (2002). As the samples are the same, any differences in the results of the numerical model can be understood as the effects of specific equations of a constitutive model and the experiments assigned to it.

The four critical responses calculated from numerical analysis are given in Table 5. Excluding linear elastic results, this table can be understood in terms of the Lade–Nelson models which resulted in the greatest values for all four critical responses. The results from the Uzan–Witczak model are the lowest, and $K - \theta$ falls in-between.

Table 5. Comparison of critical responses calculated from different models.

	Linear	$K - \theta$	Uzan–Witczak	Lade–Nelson
Case 1				
δ (mm) surface	-0.188	-0.224	-0.196	-0.294
ϵh (microstrains) bottom of AC	89.256	104.321	82.869	139.473
ϵv (microstrains) top of SG	-89.281	-96.711	-76.384	-122.194
σv (kPa) top of SG	-4.176	-4.605	-3.678	-6.068
Case 2				
δ (mm) surface	-0.178	-0.225	-0.156	-0.325
ϵh (microstrains) bottom of AC	82.172	105.145	53.319	152.726
ϵv (microstrains) top of SG	-82.422	-101.615	-44.172	-133.539
σv (kPa) top of SG	-3.867	-4.840	-2.237	-6.782
Case 3				
δ (mm) surface	-0.203	-0.262	-0.214	-0.294
ϵh (microstrains) bottom of AC	100.284	126.307	94.177	139.473
ϵv (microstrains) top of SG	-99.360	-115.904	-91.494	-122.194
σv (kPa) top of SG	-4.645	-5.598	-3.678	-4.387

It can be observed that the value of the surface deflection under load is less variable in different materials. The linear elastic analysis resulted in the measurements of 0.178–0.202 mm for three different cases of materials (0.024 mm difference). For $K-\theta$ this was from -0.224 to -0.262 mm (0.038 mm difference), for Uzan–Witczak the value changed from -0.156 to -0.214 mm (0.058 mm difference) and for the Lade–Nelson it changed from -0.294 to -0.325 mm (0.031 mm). It can be understood that the Uzan–Witczak method has a greater sensitivity to material parameters in terms of surface deflection results.

Tensile strain at the bottom of the asphalt and the vertical strain on the top of the subgrade are the key parameters in the calculation of fatigue repetition and rutting in the design of flexible pavement codes (AUSTROADS, 2004), respectively. Here, looking at the range of differences in the different constitutive models regarding the changes in the material, it can be stated that the same trends of sensitivity for the constitutive models are observable. Uzan–Witczak shows the most variation and Lade–Nelson shows the least variation.

Here it should be noted that in all four constitutive models it is only that of Lade–Nelson which also considers the effects of Poisson’s ratio on the resilient modulus.

Figures 5–7 illustrate the normalised value of critical responses calculated from four constitutive models for three cases of material parameters. Here the results are divided by the values calculated from the linear analysis in order to have a more effective comparison in terms of the actual effect of each model.

Figure 5 represents the results of four normalised critical responses for the material parameters in Case 1. Here the largest difference is related to the Lade–Nelson model. The surface deflection and horizontal strain calculated from this model is 56% larger than the linear elastic calculation. In the $K-\theta$ model, the highest difference is 19% for the calculated surface deflection and for Uzan–Witczak it is the vertical strain that shows a -14% difference. However, it should be noted that the Uzan–Witczak values are lower than values from the linear analysis with the exception of the value for surface deflection.

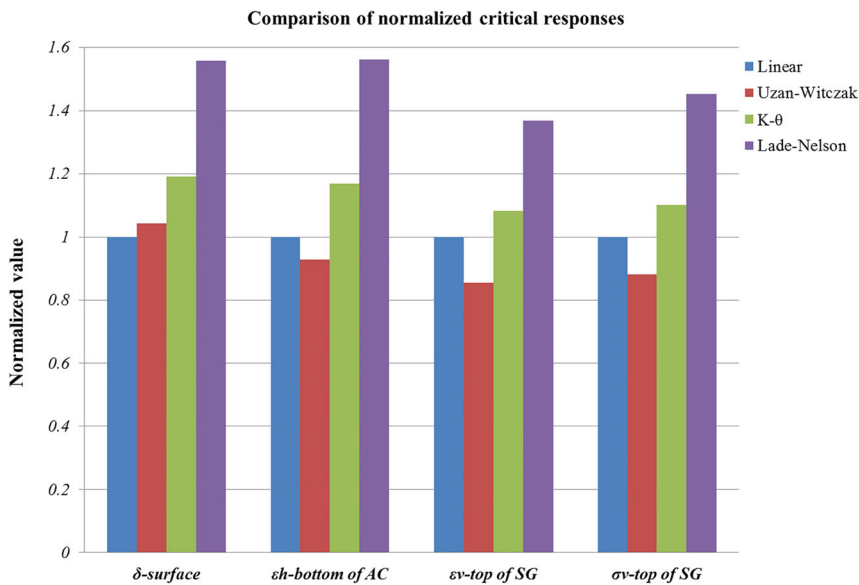


Figure 5. Comparison of the normalised critical response for Case 1.

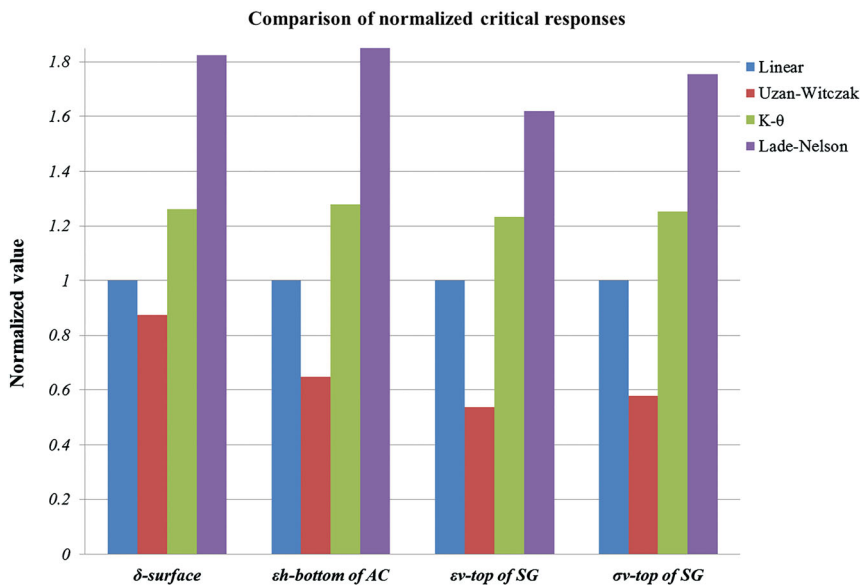


Figure 6. Comparison of the normalised critical responses for Case 2.

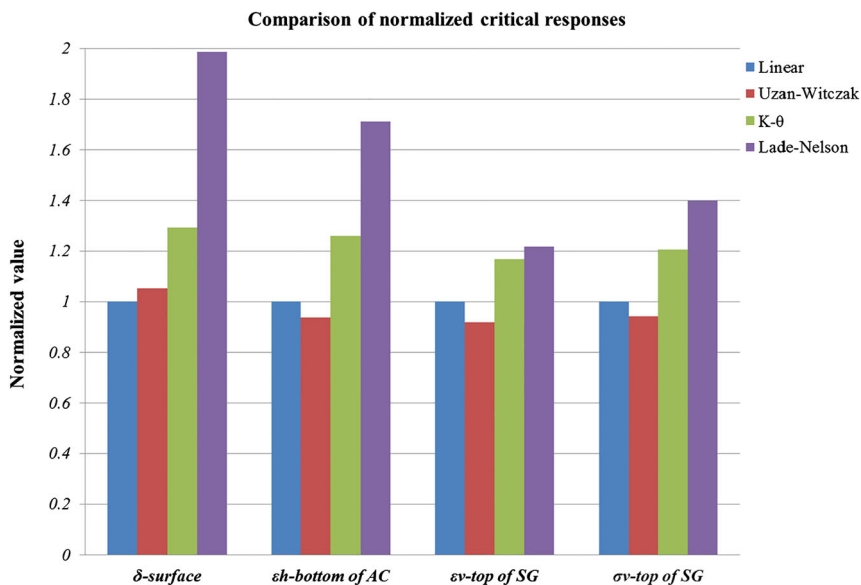


Figure 7. Comparison of the normalised critical responses for Case 3.

The results of the material parameters for Case 2 are presented in Figure 6. In this case (where the material has a stiffer Young’s modulus and a larger Poisson’s ratio compared to Case 1) the greatest difference calculated is again for Lade–Nelson. Here the greatest difference occurred with regard to the horizontal strain at the bottom of the asphalt layers and it reached up to an 86% larger value from the linear elastic calculation. This is a very significant difference and in particular it could have a critical effect on the calculation of the allowable number of repetitions for fatigue. The difference calculated for the $K - \theta$ model was between 23% (for the vertical strain

of the subgrade) and 27% (for the horizontal strain of the asphalt layer) which is comparable to that calculated in Case 1 for this model.

The calculated difference for Uzan–Witczak in this case is from -46% (vertical strain of subgrade) to -13% (surface deflection). The point which should be mentioned here is that the dependency of the Lade–Nelson model on Poisson’s ratio has a significant effect here. Referring to Table 4, it can be seen that Case 2 has a higher value of Young’s Modulus and a higher value of Poisson’s ratio (308 Mpa, 0.4) than Case 1 (240 Mpa, 0.34). However, the effects of Poisson’s ratio can only be seen in the Lade–Nelson model, while the other three constitutive models completely neglect this effect. Therefore, this great difference can be understood as being due to the nature of the constitutive model equation in Lade–Nelson.

The calculated results for the material parameters in Case 3 are illustrated in Figure 7. The highest difference is again related to Lade–Nelson reaching 99% larger values (almost double) for the surface deflection. The values for $K - \theta$ changed from 17% (vertical strain of subgrade) to 29% (surface deflection) and the range of difference for Uzan–Witczak was from -8% (vertical strain of subgrade) to 5% (surface deflection).

Mechanical behaviour of the granular layer with different constitutive models

It is of interest to consider making comparisons regarding the increasing trend of the modulus during the incremental loading. Figures 8–10 represent these trends in three cases.

The x -axis in these figures shows the increments of analysis where load increases linearly from 0% to 100% of tyre pressure during the increments. As mentioned previously, in the ABAQUS programme the load is applied with differing increments. The resilient modulus in nonlinear constitutive models is a function of the stress state, the modulus then varies in each increment for all of the elements of base layer. However, the increasing trend of a point in the centre of the loading at the top of the base layer has been selected for representation here.

Figure 8 shows the increasing trends for the materials in Case 1. As can be observed, all of the nonlinear constitutive models have a final value which is less than the value of the linear model

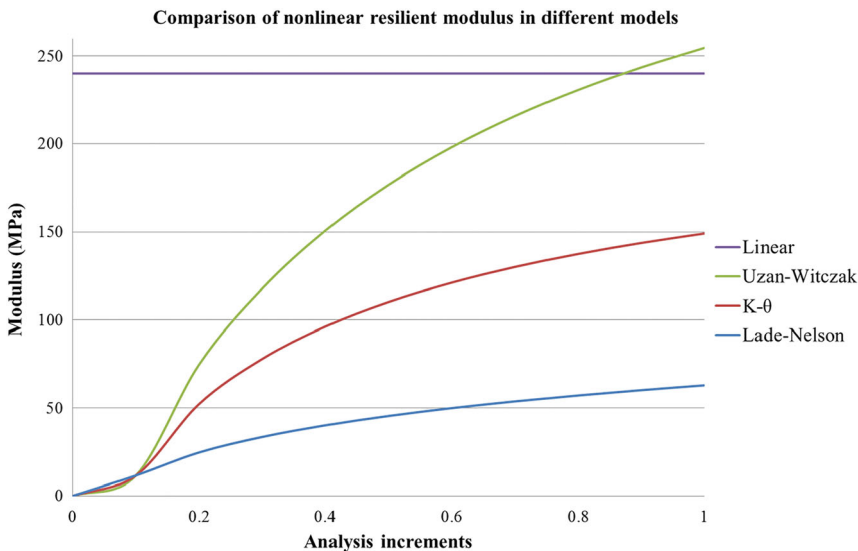


Figure 8. Increase in the nonlinear resilient modulus at the top of base layer regarding the analysis increments – Case 1.

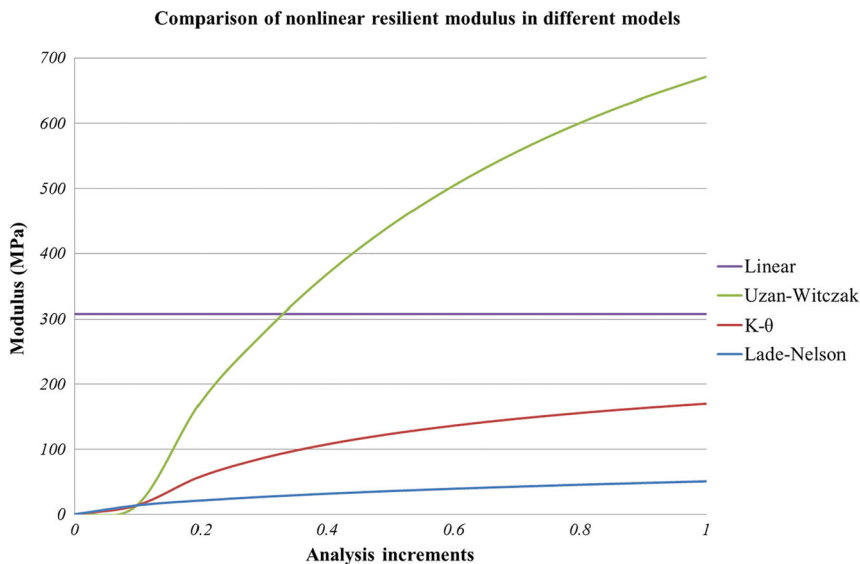


Figure 9. Increase in the nonlinear resilient modulus at the top of base layer regarding the analysis increments – Case 2.

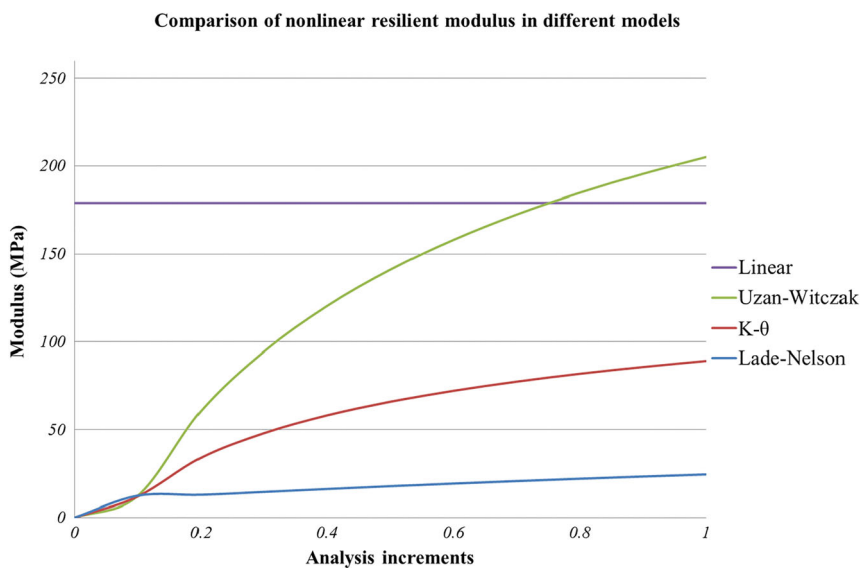


Figure 10. Increase in the nonlinear resilient modulus at the top of base layer regarding the analysis increments – Case 3.

except for Uzan–Witczak. The Lade–Nelson model shows the lowest trends and final values in this case, and the $K - \theta$ falls between that of Lade–Nelson and Uzan–Witczak.

Compared to Case 1, Case 2 shows that differences in trends have increased significantly. As shown in Figure 9, Uzan–Witczak passed the linear elastic modulus after the first few increments. In contrast, Lade–Nelson showed a very slight increasing trend in this case. The contribution of Poisson’s ratio to the constitutive model of Lade–Nelson has clearly affected this trend.

Effect of Material in Case 3 has been illustrated in Figure 10. The value of modulus calculated from Uzan–Witczak has passed the linear elastic modulus in 70% of loading increments. As the other cases Uzan–Witczak has the highest value, then the linear elastic modulus following by $K - \theta$ and Lade–Nelson.

It is worth mentioning that Uzan–Witczak has the highest range of variation with respect to material change. This can also be understood from the results presented in Table 5. It can also be concluded that the Uzan–Witczak model has a rapidly increasing trend due to increasing stresses. This is because of the nature of the exponential function of Uzan–Witczak. Comparing equations 1, 2 and 4, it can be seen that $K - \theta$ is independent of deviatoric stress, Uzan–Witczak has two terms (depending on bulk and deviatoric stress simultaneously) which multiply and intensify each other, and Lade–Nelson has two terms (depending on bulk and deviatoric stress) but these terms do not multiply.

Increasing stiffness of the base layer also leads to an increase in calculated stress in the layer itself. In Figures 11–13, the distribution of vertical stress across the depth of the base layer is presented for three cases.

In material Case 1, the calculated stress distribution in depth for Uzan–Witczak, linear elastic and $K - \theta$ are roughly similar (Figure 11) while the Lade–Nelson model has less potential to bear vertical stresses. Here, with Uzan–Witczak, the stress varies from -56 kPa at the top of the base to -5 kPa at the bottom. The variation range for the linear model is from -49 to -6 kPa. For $K - \theta$ this range is from -43 to -6 kPa. It is clear that the variation in these three models demonstrates a relatively close relationship (-56 to -43 kPa at top and -6 to -5 kPa at the bottom). However, a considerable difference is presented in Lade–Nelson where the stress varies from -27 to -8 kPa. Moreover, the stress distribution of Lade–Nelson is more uniform than in the other three models.

In Figure 12, the stress distribution of material Case 2 is presented. The three models here show different results. The calculated vertical stress for Uzan–Witczak is -85 kPa at the top and -5 kPa at the bottom of the base layer. These values for the linear model are -55 to -5

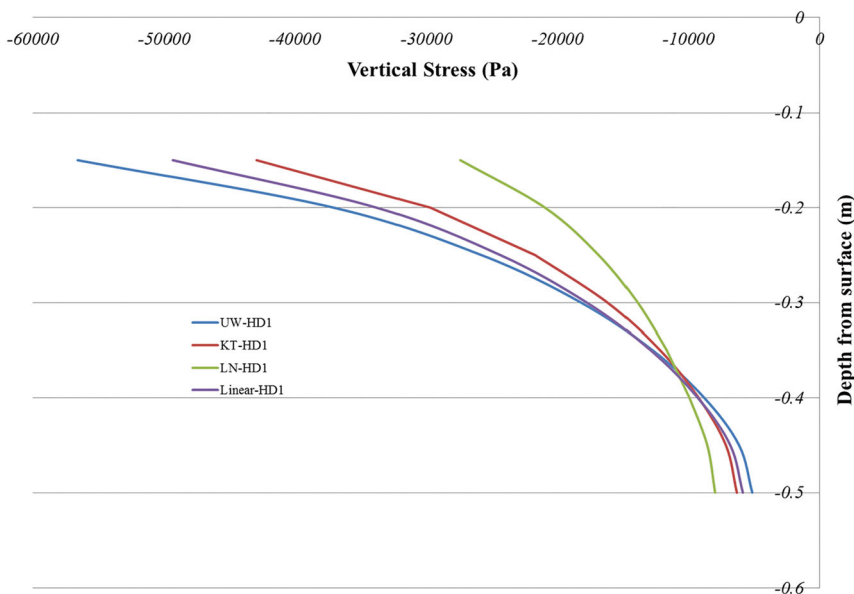


Figure 11. Distribution of vertical stress in base layer – Case 1.

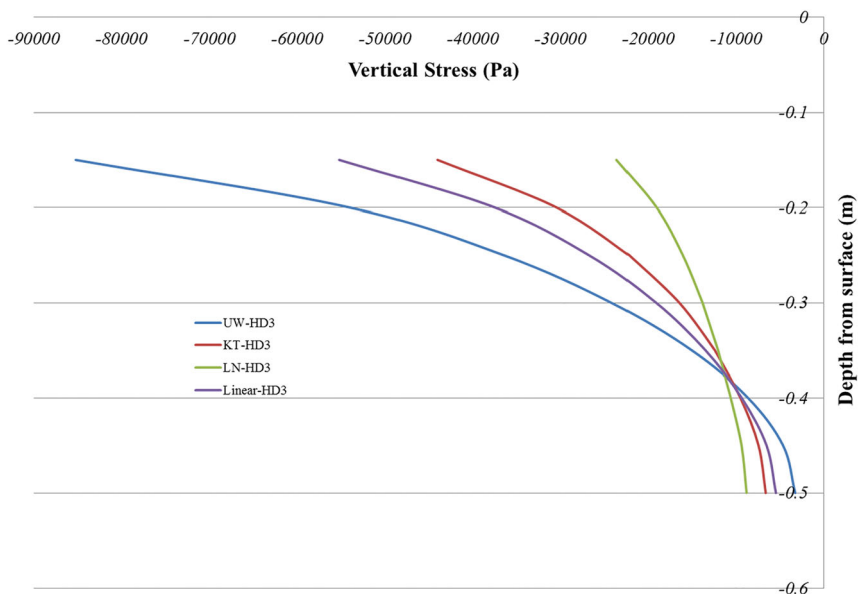


Figure 12. Distribution of vertical stress in base layer – Case 2.

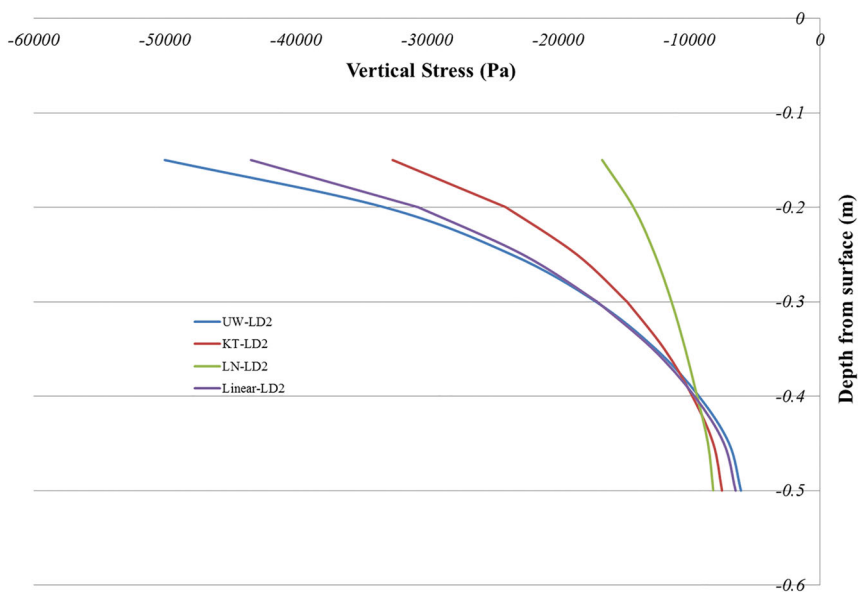


Figure 13. Distribution of vertical stress in base layer – Case 3.

kPa and for $K - \theta$ they are -45 to -7 kPa. Finally, the vertical stress values for the Lade–Nelson model are -23 kPa at the top and -9 kPa at the bottom. Therefore, the variation of results among the three models is greater than those observed in Case 1. Moreover the results of Lade–Nelson show a stronger trend to more uniform distribution.

In Figure 13, the vertical stress distribution for material Case 3 is illustrated. Here the range of values for different models is as follows: -50 to -6 kPa for Uzan–Witczak, -43 to -6 kPa

for linear elastic, -32 to -7 kPa for $K-\theta$ and -16 to -8 kPa. From these results it can be understood that in going to the depth of the base layer, the results of the vertical stress distribution calculated from Uzan–Witczak have more similarity to the linear elastic results. Moreover the calculated results from Lade–Nelson are more uniform compared to the two previous cases (Cases 1 and 2).

To gain a better understanding of how the vertical modulus has been distributed in the base layer, the contours of the modulus at the top and inside of the base layer are presented.

To calculate the vertical modulus of the base layer, Equation (12) was used:

$$E_z = \frac{\sigma_{zz}^n}{\varepsilon_{zz}^n}, \tag{11}$$

where E_z represents the vertical modulus in the final increment (increment number n) and z is the direction of the depth of the model. For this reason, when the calculated strain is too small (near zero), a high value of E_z can be virtually calculated, while this very stiff calculated value is not a meaningful value and should be neglected. This will happen when the strains are out of the area around the loading wheels. Therefore the calculated values for contours in the area outside the loading wheels should be considered with caution.

Figures 14 demonstrates the distribution of the vertical elastic contours at the top of the base layer in the $X - Y$ plan (wheel axle is parallel to Y -axis) for material Case 1.

The contours relating to $K-\theta$, Lade–Nelson and Uzan–Witczak are presented, respectively. Comparing these three contours reveals that in the Lade–Nelson model the modulus is more uniformly distributed between the two loading wheels. In the $K-\theta$ model, clear contour lines can be distinguished which indicates an uneven distribution of the vertical elastic modulus between loads. For Uzan–Witczak, the values are distributed extremely unevenly (having a maximum value beneath the centre of the load and a lower value between the wheels).

The distribution of the vertical modulus in the depths of the base layer is another point worthy of consideration. Figure 15 demonstrates this distribution for materials Case 1 in $K-\theta$, Lade–Nelson and Uzan–Witczak.

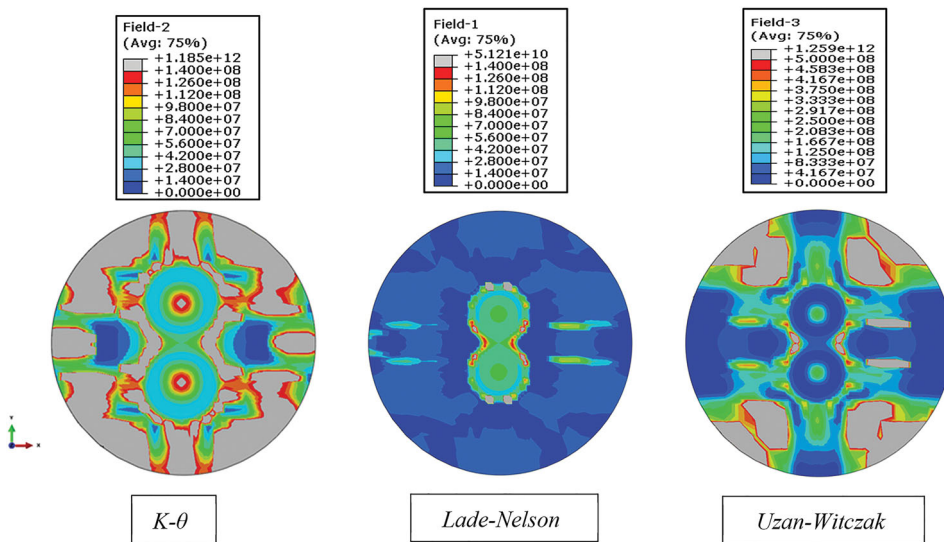


Figure 14. Contours of resilient modulus in plane at the top of base layer for different models.

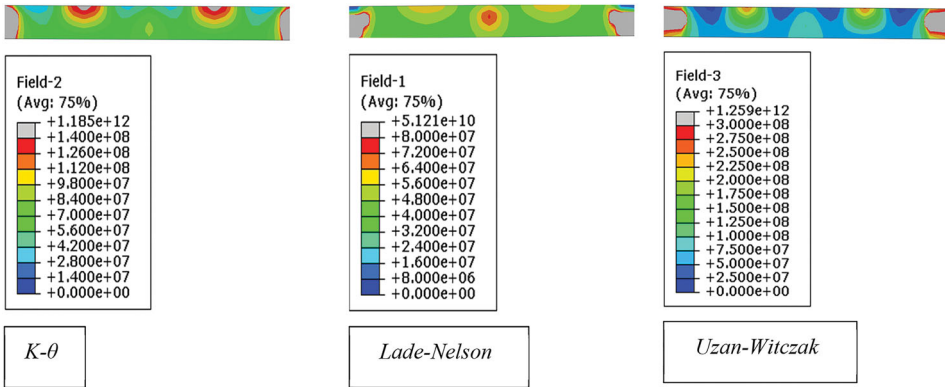


Figure 15. Contours of resilient modulus in the depths of base layer for different models between two wheels.

Comparing these three constitutive models, it can be understood that the uniformly distributed elastic modulus occurred again in Lade–Nelson, and this distribution is severely uneven for Uzan–Witczak. In Uzan–Witczak, the elastic modulus increased in a column-like way beneath the centre of the load (Figure 15). Another interesting phenomenon is the formation of stiffer materials (higher elastic modulus) between the two wheels. This occurred in all three cases. However, this can be seen more clearly in Lade–Nelson (Figure 15) where the highest value of the elastic modulus actually occurred not beneath the load but in an area between the two wheels. It should be noted that geometry of loading tyre and the tyre pressure define the stress field. On the other hand, the resilient modulus is defined as a function of stress field. Therefore it should be noted that the stiffer behaviour of granular is expected where there is higher stress.

Discussion

As an overall comparison, some of the major points can be further discussed. First, the implementation of the Uzan–Witczak model resulted in a general “stiffer” behaviour than that in other constitutive models (including linear elastic). Here the word “stiff” refers to less deformation (deflection and strain) against the applied pressure. In this regard, Lade–Nelson has the “softest” behaviour (Table 5 and Figures 5–7). The stiffness can be related to the trend of the development of the elastic modulus with respect to an increasing load increment and accordingly, stresses in the base layer. Here again the rate of increase in the elastic modulus of Uzan–Witczak is higher than that in the other constitutive models (Figures 8–10). This is due to the dependency of the Uzan–Witczak constitutive equation on both bulk stress and deviatoric stress (Eq. (3)). Although the Lade–Nelson model is also dependent upon these two, the nature of the equation is different from that of Uzan–Witczak. In Lade–Nelson, the two terms are simply added to each other, while in Uzan–Witczak these two terms are multiplied and therefore they greatly intensify the effect of the increasing stress. Another cause of the stiffer behaviour of Uzan–Witczak can be explained when the development of stress in the base is investigated. Calculations showed that having a higher elastic modulus in loading increments leads to higher stress in the same layer. Considering the dependency of the modulus on the stress values this itself results in a higher elastic modulus. This demonstrates another reason for the “stiffer” behaviour in Uzan–Witczak (Figures 11–13).

Consideration of the distribution of the elastic modulus according to the equation of the constitutive model explains the actual mechanical effect of each model. In this study, it can be seen that the Uzan–Witczak model forms a high elastic modulus column beneath the load centre, while

in the Lade–Nelson model, the elastic modulus is more uniformly distributed between the two wheels. This means that the Uzan–Witczak model has a major value for the stress of the loading wheel in the area beneath the wheels. In other words, in this model the stress has little distribution in a lateral direction, while in Lade–Nelson the lateral distribution of stress is more considerably developed. The distribution of the elastic modulus from the $K - \theta$ model is not as uniform as that of Lade–Nelson and not as localised as Uzan–Witczak. Moreover, in all models there is a localised high modulus area between the loading wheel, and this area is more distinguishable in Lade–Nelson.

Finally, it should be noted that although changes in the asphalt and subgrade properties (including thickness and material properties) will produce different results, the trend in mechanical behaviour is expected to be the same regarding the implementation of constitutive models. Therefore, stiffer responses (as mentioned before) can be expected from Uzan–Witczak, and more uniformly distributed responses can be expected from Lade–Nelson in any of the cases. Among all of the models, it is deemed that Uzan–Witczak model represents the response of granular materials in more proper way. The reason is that it can consider both deviatoric and confined pressure into account. The Uzan–Witczak model has been accepted more widely among the researchers with the same reason (e.g. Attia & Abdelrahman, 2011; González et al., 2007).

Conclusion

Three different nonlinear constitutive equations for the resilient modulus of granular material used in the base layer of flexible pavement were compared to each other, and a linear elastic analysis conducted. A sample layered flexible pavement was modelled three dimensionally and the constitutive models were implemented in the ABAQUS finite-element programme through UMAT subroutines. To consider the effect of material variation three different material parameters were considered. The results of the analysis indicated that the constitutive model proposed by Uzan–Witczak resulted in the lowest responses in terms of surface deflection and horizontal strain at the bottom of the asphalt layer. The Lade–Nelson model illustrated the largest values compared to other models, and the results calculated from $K - \theta$ fall in-between these two. The increase in the elastic modulus with respect to loading increments is larger in the Uzan–Witczak model and smaller in the Lade–Nelson model. Moreover, the distribution of the elastic modulus is highly localised around the loading wheels in Uzan–Witczak but it is more uniformly distributed in Lade–Nelson.

Acknowledgements

Authors acknowledge the Australian Research Council (ARC) financial support to this research under the ARC Scheme (LP110100634), conducted at the Department of Civil Engineering, Curtin University. Author also acknowledges financial contribution of Australian Asphalt Pavement Association and Canning City Council in this research.

Disclosure statement

No potential conflict of interest was reported by the authors.

Funding

This work was supported by Australian Research Council (ARC) [LP110100634].

ORCIDBehzad Ghadimi  <http://orcid.org/0000-0001-6299-7617>**References**

- AASHTO. (1993). *Guide for design of pavement structures*. Washington, DC: American Association of State Highway and Transportation Officials.
- Araya, A. A., Huurman, M., Houben, L. J., & Molenaar, A. A. (2011). *Characterizing mechanical behavior of unbound granular materials for pavements*. Paper presented at the Transportation Research Board 90th annual meeting.
- Araya, A. A., Huurman, M., Molenaar, A. A., & Houben, L. J. (2012). Investigation of the resilient behavior of granular base materials with simple test apparatus. *Materials and Structures*, 45(5), 695–705.
- Attia, M., & Abdelrahman, M. (2011). Effect of state of stress on the resilient modulus of base layer containing reclaimed asphalt pavement. *Road Materials and Pavement Design*, 12(1), 79–97.
- Austrroads. (2004). *Pavement design – a guide to the structural design of road pavements*. Sydney: Author.
- Bodhinayake, B. C. (2008). *A study on nonlinear behaviour of subgrades under cyclic loading for the development of a design chart for flexible pavements* (University of Wollongong Thesis Collection, 868).
- Burmister, D. M. (1945). The general theory of stresses and displacements in layered systems. I. *Journal of Applied Physics*, 16(2), 89–94.
- Burmister, D. M., Palmer, L., Barber, E., Casagrande, A. D., & Middlebrooks, T. (1943). *The theory of stress and displacements in layered systems and applications to the design of airport runways*. Paper presented at the Highway Research Board Proceedings.
- Cho, Y. H., McCullough, B. F., & Weissmann, J. (1996). Considerations on finite-element method application in pavement structural analysis. *Transportation Research Record: Journal of the Transportation Research Board*, 1539(-1), 96–101.
- Cortes, D., Shin, H., & Santamarina, J. (2012). Numerical simulation of inverted pavement systems. *Journal of Transportation Engineering*, 138(12), 1507–1519.
- Duncan, J. M., Monismith, C. L., & Wilson, E. L. (1968). Finite element analyses of pavements. *Highway Research Record Highway Research Board*, 228, 18–33.
- Fahey, M., & Carter, J. P. (1993). A finite element study of the pressuremeter test in sand using a nonlinear elastic plastic model. *Canadian Geotechnical Journal*, 30(2), 348–362.
- Gedafa, D. S. (2006). *Comparison of flexible pavement performance using kenlayer and hdm-4*. Ames, IA: Midwest Transportation Consortium.
- González, A., Saleh, M., & Ali, A. (2007). Evaluating nonlinear elastic models for unbound granular materials in accelerated testing facility. *Transportation Research Record: Journal of the Transportation Research Board*, 1990(1), 141–149.
- Hadi, M., & Symons, M. (1996). Computing stresses in road pavements using CIRCLY, MSC/NASTRAN and STRAND6. Transactions of the Institution of Engineers, Australia. *Civil Engineering*, 38(2–4), 89–93.
- Hibbitt, K., & Sorensen. (2010). *ABAQUS: Analysis user's manual*, Vol. I–IV, version 6.10, Inc. Providence, RI.
- Hicks, R. G., & Monismith, C. L. (1971). *Factors influencing the resilient response of granular materials* (Highway Research Record 345).
- Hjelmstad, K., & Tacioglu, E. (2000). Analysis and implementation of resilient modulus models for granular solids. *Journal of Engineering Mechanics*, 126(8), 821–830.
- Huang, Y. (1969). *Finite element analysis of nonlinear soil media*. Paper presented at the proceedings, symposium on application of finite element methods in civil engineering (pp. 663–685). Nashville: Vanderbilt University.
- Huang, Y. H. (1993). *Pavement analysis and design*. Englewood Cliffs, NJ: Prentice-Hall.
- Kim, M. (2007). *Three-dimensional finite element analysis of flexible pavements considering nonlinear pavement foundation behavior* (Ph.D. thesis). Department of Civil Engineering, University of Illinois at Urbana-Champaign, Urbana-Champaign, IL.
- Kim, M., & Lee, J. H. (2011). Study on nonlinear pavement responses of low volume roadways subject to multiple wheel loads. *Journal of Civil Engineering and Management*, 17(1), 45–54.
- Kim, M., & Tutumluer, E. (2006). Modeling nonlinear, stress-dependent pavement foundation behavior using a general-purpose finite element program. *Geotechnical Special Publication*, 154, 29–36.

- Kim, M., & Tutumluer, E. (2010). Validation of a three-dimensional finite element model using airfield pavement multiple wheel load responses. *Road Materials and Pavement Design*, 11(2), 387–408.
- Kim, M., Tutumluer, E., & Kwon, J. (2009). Nonlinear pavement foundation modeling for three-dimensional finite-element analysis of flexible pavements. *International Journal of Geomechanics*, 9(5), 195–208.
- Lade, P. V., & Nelson, R. B. (1987). Modelling the elastic behaviour of granular materials. *International Journal for Numerical and Analytical Methods in Geomechanics*, 11(5), 521–542.
- Lee, J., Kim, J., & Kang, B. (2009). Normalized resilient modulus model for subbase and subgrade based on stress-dependent modulus degradation. *Journal of Transportation Engineering*, 135(9), 600–610.
- Mallela, J., & George, K. (1994). *Three-dimensional dynamic response model for rigid pavements* (Transportation Research Record 1448).
- Mishra, D., & Tutumluer, E. (2012). Aggregate physical properties affecting modulus and deformation characteristics of unsurfaced pavements. *Journal of Materials in Civil Engineering*, 24(9), 1144–1152.
- Rowshanzamir, M. A. (1997). *Resilient cross-anisotropic behaviour of granular base materials under repetitive loading* (Ph.D. dissertation). School of Civil Engineering, University of New South Wales, Kensington, Australia.
- Sahoo, U. C., & Reddy, K. S. (2010). Effect of nonlinearity in granular layer on critical pavement responses of low volume roads. *International Journal of Pavement Research and Technology*, 3(6), 320–325.
- Seed, H. B., Chan, C. K., & Lee, C. E. (1962). *Resilience characteristics of subgrade soils and their relation to fatigue failures in asphalt pavements*. Paper presented at the international conference on the structural design of asphalt pavements. Supplement.
- Taciroglu, E., & Hjelmstad, K. (2002). Simple nonlinear model for elastic response of cohesionless granular materials. *Journal of Engineering Mechanics*, 128(9), 969–978.
- Tutumluer, E., Little, D. N., & Kim, S. H. (2003). Validated model for predicting field performance of aggregate base courses. *Transportation Research Record: Journal of the Transportation Research Board*, 1837(-1), 41–49.
- Uddin, W., Zhang, D., & Fernandez, F. (1994). *Finite element simulation of pavement discontinuities and dynamic load response* (Transportation Research Record 1448).
- Uzan, J. (1985). *Characterization of granular material* (Transportation Research Record 1022).
- Wang, H., & Al-Qadi, I. L. (2013). Importance of nonlinear anisotropic modeling of granular base for predicting maximum viscoelastic pavement responses under moving vehicular loading. *Journal of Engineering Mechanics*, 139(1), 29–38.
- Wardle, L., Youdale, G., & Rodway, B. (2003). In ARRB transport research conference, 21st, Cairns, Queensland, Australia Road Engineering Association of Asia and Australasia.
- Witczak, M. W., & Uzan, J. (1988). *The universal airport pavement design system rep. I granular material characterization*. College Park, MD: University of Maryland.
- Worku, A. (2012). Calibrated analytical formulas for foundation model parameters. *International Journal of Geomechanics*, 13(4), 340–347.
- Zaghloul, S., & White, T. (1993). *Use of a three-dimensional, dynamic finite element program for analysis of flexible pavement* (Transportation Research Record 1388, 60–69).